Published in final edited form as:

Small. 2014 July 23; 10(14): 2830–2743. doi:10.1002/smll.201303646.

Fully-Loaded Micromotors for Combinatorial Delivery and Autonomous Release of Cargoes

Dr. Sirilak Sattayasamitsathit[†], **Huanhuan Kou**[†], **Wei Gao**, **Walter Thavarajah**, **Kevin Kaufmann**, **Prof. Liangfang Zhang**, and **Prof. Joseph Wang**

Department of Nanoengineering, University of California, San Diego, La Jolla, California 92093 USA

Liangfang Zhang: zhang@ucsd.edu; Joseph Wang: josephwang@ucsd.edu

Keywords

Self-destruction micromachines; Combinatorial drug delivery; Cargo release; Zinc; Drug delivery

Nano/micromotors are tiny synthetic devices that can effectively convert energy into movement and forces.[1-6] Operating on locally supplied fuels, such as hydrogen peroxide, acid, and even water,[7-10] these artificial motors can perform considerably complex tasks.[3-5] For instance, hydrogen-peroxide powered micromotors have shown a remarkable ability to isolate circulating tumor cells and bacteria from raw biological fluids.[11,12] Previous studies have also demonstrated that by attaching drug-loaded nanoparticles onto the outer surface of micromotors, the motors can deliver their therapeutic payloads to a target destination through pre-defined paths with a speed over three orders of magnitude higher than regular Brownian motion, reflecting the large propelling and towing forces of the motors.[13] Along with remarkable control over the movement directionality, these man-made microscale devices are currently a subject of intense fundamental and practical research activities.[4] While still in an early stage, attempts to explore biomedical applications of micromotors are extremely active and encouraging.[3-5]

Delivering cargoes in a defined and fast manner represents a major application of synthetic micromotors.[13,14] The key challenge, however, is how to design, fabricate, and optimize new motors with appropriate functions for effective delivery and efficient release of their payloads. A reliable delivery vehicle is expected to have the capability for carrying a large amount of cargoes for enhanced effectiveness (e.g., therapeutic efficacy in drug delivery), delivering simultaneously different types of cargoes for multitasking (e.g., theranostics or combination therapy to overcome drug resistance), releasing payloads in a responsive manner (e.g., controlled drug release), and destroying itself when no longer needed.[15-18] To meet these critical multifunctionality requirements, we successfully constructed in the

Correspondence to: Liangfang Zhang, zhang@ucsd.edu; Joseph Wang, josephwang@ucsd.edu.

[†]These authors contributed equally to this work.

Supporting Information

Supporting Information is available from the Wiley Online Library or from the author.

present study a novel chemically-powered zinc-based micromotor that displays impressive cargo loading, delivery, and release capabilities.

The fully-loaded double-conical zinc micromotors are fabricated by coupling template-electrodeposition with particle-infiltration techniques using silica and gold nanoparticles as model cargo analogues. As illustrated in Figure 1, the motor fabrication route involves the electrodeposition of zinc within the conical micropores of a polycarbonate membrane which are tightly packed with the cargo particles. Dissolution of the membrane template results in the release of the freestanding double-conical shaped micromotors, characterized with a remarkably high cargo packing fraction of up to 74% of the entire motor body (for mono-sized spherical cargoes according to Kepler conjecture).[19] This loading fraction can be further increased by combining different sized spherical particles or using particles with different shapes. When the micromotors are placed in acidic fuel media, hydrogen bubbles are spontaneously ejected from one end, leading to a bubble thrust and a fast movement (Figure 1e and Movie S1). Such directional locomotion is enabled by the formation of a galvanic cell between the zinc and the sputtered gold contact.[20] The dissolution of the zinc body leads to an autonomous release of the encapsulated cargoes and eventual splitting apart of the motors (Figure 1f), while the motors are moving till they are almost fully dissolved.

The scanning electron microscopy (SEM) images demonstrate the morphology of the template-prepared Zn micromotors loaded with monodisperse SiO_2 nanoparticles (diameter ~500 nm) (Figure 2a,b). Infiltrating the cargo spheres within the micropores of the membrane template allows for convenient and efficient cargo encapsulation within the electrodeposited zinc without any chemical linking steps. The resulting cargo-loaded micromotors are 20 μm long and have a double-cone structure (with 2 μm diameter at both ends and 1 μm diameter in their center), reflecting the shape of the micropores of the polycarbonate membrane template. These SEM images illustrate that the SiO_2 particles are tightly packed (with minimal gaps) and fully-loaded within the body of the zinc micromotors. As expected, only a small portion of the particles is visible on the outside of the fully-loaded Zn body (Figure 2b). The corresponding energy-dispersive X-ray spectroscopy (EDX) data indicates that the SiO_2 particles are dispersed uniformly and densely throughout the entire micromotor body, with zinc deposited in the voids between these cargo particles (Figure 2c,d). Control experiments were carried out using zinc micromotors without the SiO_2 particles. SEM images (Figure 2e,f) and EDX examination (Figure 2g,h) confirm that only elemental zinc is present in these control micromotors.

Next, we demonstrated the capabilities of the zinc micromotors for combinational cargo delivery and multifunctional operation. For this purpose, the micromotors were successfully loaded with a binary cargo mixture of different sizes and types of nanoparticles. As illustrated in Figure 3a, such simultaneous encapsulation of different cargo populations was tested using SiO_2 nanoparticles of different sizes (500 nm and 250 nm in diameter), as well as co-encapsulation of Au nanoparticles (diameter ~20 nm) and SiO_2 nanoparticles (diameter ~500 nm). As shown in Figure 3b and c, the top and side-view SEM images of the micromotors clearly indicate a homogeneous full loading of 500 nm and 250 nm SiO_2 particles within the motors. The SEM image (Figure 3d) and EDX mapping (Figure 3e-g) further confirm that the zinc micromotors can be fully loaded with 20 nm Au nanoparticles

together with 500 nm SiO_2 particles. Furthermore, the EDX mapping analysis shows the uniform distribution of elemental Au and Si over the entire body of the micromotor. Note that the Au nanoparticles cannot be observed in the SEM image owing to their small size. The SEM image (Figure 3h) and EDX mapping (Figure 3i-k) of the control zinc micromotors (without particle loading) confirm the absence of Au and Si within the zinc body of the micromotors. Collectively, these results demonstrate that the micromotor preparation route allows convenient packing of multicomponent cargoes at predetermined sizes, compositions and proportions.

Since the maximum packing capacity for mono-sized spheres is 74% of the total container volume according to Kepler conjecture,[19] the maximum packing capacity of 250 and 20 nm diameter cargo spheres within the 36.7 μm^3 volume of the double-cone micromotor is estimated to be slightly over 3,000 and 6,000,000 particles per micromotor, respectively. However, as the particle size increases, the container wall has a greater influence on the packing arrangement of the particles and increases the void volume within the micromotor. By packing the micromotors with two populations of nanoparticles of greatly different sizes (e.g., 20 and 500 nm, as the case in Figure 3d), it is likely to have a packing fraction higher than 74%, because smaller cargoes can fill the voids between larger cargoes. Moreover, changing to non-spherical nanoparticle shapes, such as hexagons, may further increase the packing capacity.

Such high particle loading capacity and new functionalities do not compromise the locomotion behavior of the motors. For example, the time-lapse images in Figure 4a (corresponding to Movie S2) show the effective movement of several zinc micromotors fully-loaded with SiO_2 nanoparticles (500 nm in diameter) in a strongly acidic environment and the concomitant cargo release from the motors. The cargo-loaded micromotors are self-propelled with an average initial speed of 110 $\mu m\ s^{-1}$ in a 0.7 M HCl solution while the speed of Zn micromotors without cargoes is around 180 $\mu m\ s^{-1}$ under the same conditions. A hydrogen bubble tail generated from one side of the micromotor is clearly observed (Figure 4a, 0 s). As their zinc body is oxidized and dissolved by the acid fuel, the cargoes are released autonomously. Such gradual zinc dissolution leads to the breaking apart of the motors at their narrow center region, and eventually to a complete release of the encapsulated cargoes (Figure 4a, 6-9 s). Within less than 15 sec, the micromotors stop their motion and nearly disappear (Figure 4a, 12 s). To better illustrate the cargo release process, we intentionally stopped the motion of the motors by reducing the fuel (acid) concentration and then focused on a single stationary micromotor with higher magnification. It was shown that the motor started to break apart 3 s after adding the acid, leading to the release of a large amount of cargo particles, and to complete dissolution of the motors (Figure 4b and Movie S3).

The speed and life time of the acid-powered micromotors are strongly dependent on the concentration of the surrounding acid and upon their payload loading fraction. Increasing speed of fully-loaded micromotors from 110 to 140 $\mu m\ s^{-1}$ can be achieved by increasing HCl concentration from 0.7 M to 1 M, however resulting in a shorter lifetime from 15s to 5s. The zinc micromotors without SiO_2 particle loading are self-propelled in the 0.7 M HCl solution at a speed of 180 $\mu m\ s^{-1}$, which corresponds to a relative speed of 8 body lengths

s^{-1}. In contrast, the SiO_2-loaded micromotors are moving at a slower speed of 110 μm s^{-1} (5.5 body lengths s^{-1}). SiO_2-loaded micromotors here is slower than Zn-polyaniline reported previously (100 body lengths s^{-1}) owing to their solid structure (no opening) and being fully packed with SiO_2 nanoparticles. We also demonstrated that lifetime of cargo-loaded micromotors was affected by the amount of payloads in the micromachines. The cargo-loaded motors are fully destroyed in this solution within 15 s, as compared to the 20 s lifetime of the control motors which have higher zinc content.

In summary, an attractive self-propelled microscale motor has been developed that concurrently possesses multiple functions for potential biomedical applications, including a remarkably high loading capacity, combinatorial delivery of different cargoes and autonomous ‘on-the-fly’ release of payloads. Moreover, unlike most existing micromotors that are designed to withstand deterioration, these new micromotors destroy themselves upon completing their delivery mission. While the concept was illustrated through the loading of model SiO_2 and Au nanoparticle cargoes, it could be readily expanded to simultaneous encapsulation of a wide variety of payloads possessing different biomedical functions such as therapy, diagnostics, and imaging. This development is thus expected to advance significantly the emerging field of cargo- towing nano/micromotors and to further expand the opportunities for biomedical applications of nano/microvehicles.

Experimental Section

Fully-Loaded Micromotors

Detailed motor fabrication and characterization protocols used in this study can be found in Supplementary Data 1. Briefly, cargo-loaded Zn micromotors were fabricated using a membrane-template directed electrodeposition method in the microparticle-infiltrated polycarbonate membrane. The Cyclopore polycarbonate membranes (Whatman 7060-2511) containing 2 μm diameter pores with a 75 nm gold sputtered film were used for cargo packing. Diluted 60 and 15 fold SiO_2 particles were filled into the membrane pore by vacuum infiltration. The size of the micromotors was controlled by the pore size of the membrane template and the deposition charge. Cargo-loaded micromotors were synthesized by mechanically packing SiO_2 particles (diameter of 500 nm) in the membrane templates,[13,14] followed by the zinc electrodeposition process using a potential of -1.2 V for a total charge of 8 C. Mixture of Au nanoparticles (20 nm) with SiO_2 microparticles (500 nm) or 2 different sizes of SiO_2 particles (500 and 250 nm) were used for simulating multi-cargo loaded micromotors. The micromotors were released from the template by mechanical polishing and membrane dissolution in methylene chloride. The samples were washed with methylene chloride, ethanol and water two times of each and were collected by centrifugation.

Micromotors characterization

The morphology of the double-conical micromotors and the distribution of embedded cargos were examined by Scanning electron microscopy (SEM) imaging and Energy-dispersive X-ray (EDX) analysis. For long term storage of micromotors, they should be preserved in ethanol to prevent degradation. The propulsion and controlled payload release of cargo-

loaded micromotors were examined in acidic solutions containing 0.3-1.0 M HCl (along with 1.7% Triton X-100). Real-time videos of propulsion of the cargo-loaded micromotors, autonomous release of payloads and self-destruction were recorded using an inverted optical microscope (Nikon Instrument Inc. Ti-S/L100), coupled with a 40x objective lens, and a Hamamatsu digital camera C11440 using the NIS-Elements AR 3.2 software.

Supplementary Material

Refer to Web version on PubMed Central for supplementary material.

Acknowledgments

This project received support from the Defense Threat Reduction Agency-Joint Science and Technology Office for Chemical and Biological Defense (Grant no. HDTRA1-13-1-0002). L. Z. acknowledges the funding support from the National Institute of Diabetes and Digestive and Kidney Diseases of the National Institutes of Health under Award Number R01DK095168. H. K. acknowledges the China Scholarship Council (CSC) for the financial support. W.G. is a HHMI International Student Research fellow.

References

1. Mallouk TE, Sen A. Sci Amer. 2009; 300:72. [PubMed: 19438052]
2. Ozin GA, Manners I, Fournier-Bidoz S, Arsenault A. Dream nanomachines. Adv Mater. 2005; 17:3011.
3. Wang J, Gao W. ACS Nano. 2012; 6:5745. [PubMed: 22770233]
4. Wang, J. Nanomachines: Fundamentals and Applications. Wiley-VCH; Weinheim, Germany: 2013.
5. Sengupta S, Ibele ME, Sen A. Angew Chem Int Ed. 2012; 51:8434.
6. Mei Y, Solovev AA, Sanchez S, Schmidt OG. Chem Soc Rev. 2011; 40:2109. [PubMed: 21340080]
7. Paxton WF, Kistler KC, Olmeda CC, Sen A, St Angelo SK, Cao Y, Mallouk TE, Lammert PE, Crespi VH. J Am Chem Soc. 2004; 126:13424. [PubMed: 15479099]
8. Mei YF, Huang G, Solovev AA, Ureña EB, Mönch I, Ding F, Reindl T, Fu RKY, Chu PK, Schmidt OG. Adv Mater. 2008; 20:4085.
9. Gao W, Uygun A, Wang J. J Am Chem Soc. 2012; 134:897. [PubMed: 22188367]
10. Gao W, Pei A, Wang J. ACS Nano. 2012; 6:8432. [PubMed: 22891973]
11. Balasubramanian S, Kagan D, Hu CJ, Campuzano S, Lobo-Castañon MJ, Lim N, Kang DY, Zimmerman M, Zhang L, Wang J. Angew Chem Int Ed. 2011; 50:4161.
12. Campuzano S, Orozco J, Kagan D, Guix M, Gao W, Sattayasamitsathit S, Claussen JC, Merkoçi A, Wang J. Nano Lett. 2012; 12:396. [PubMed: 22136558]
13. Kagan D, Laocharoensuk R, Zimmerman M, Clawson C, Balasubramanian S, Kang D, Bishop D, Sattayasamitsathit S, Zhang L, Wang J. Small. 2010; 6:2741. [PubMed: 20979242]
14. Gao W, Kagan D, Pak O, Clawson C, Campuzano S, Chuluun-Erdene E, Shipton E, Fullerton EE, Zhang L, Lauga E, Wang Joseph. Small. 2012; 8:460–467. [PubMed: 22174121]
15. Zhang L, Gu FX, Chan JM, Wang AZ, Langer RS, Farokhzad OC. Clin Pharmacol Ther. 2008; 83:761. [PubMed: 17957183]
16. Davis ME, Chen ZG, Shin DM. Nat Rev Drug Discov. 2008; 7:771. [PubMed: 18758474]
17. Shi J, Xiao Z, Kamaly N, Farokhzad OC. Acc Chem Res. 2011; 44:1123. [PubMed: 21692448]
18. Hu CM, Zhang L. Biochem Pharmacol. 2012; 83:1104. [PubMed: 22285912]
19. Hales TC. Ann Math. 2005; 162:1065.
20. Roberge, PR. Handbook of Corrosion Engineering. McGraw-Hill Professional; New York, USA: 2000.

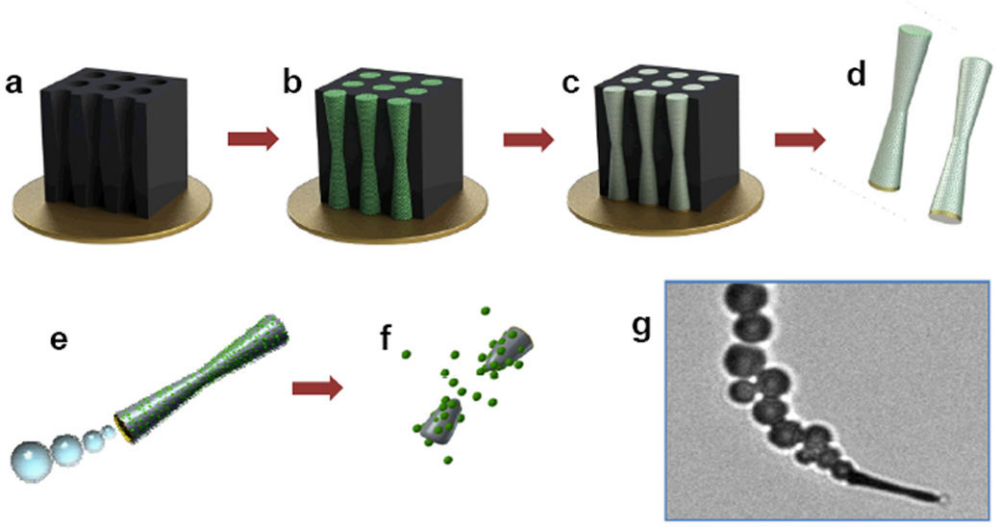

Figure 1.

Dual-template fabrication of the fully-loaded zinc-based micromotors. (a) sputtering membrane template with a gold conducting layer; (b) packing nanoparticle cargoes into the membrane pores; (c) electrodeposition of zinc into the biconical pores; (d) dissolution of the membrane template to release individual micromotors; (e-f) hydrogen-bubble propulsion in acid and autonomous release of the cargoes while the motors are dissolved and destroyed; (g) microscopic image of a bubble-propelled cargo-loaded micromotor in HCl (Movie S1).

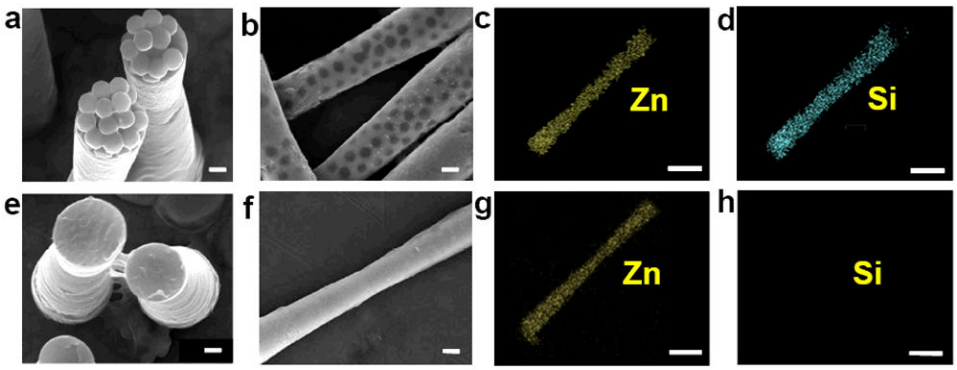

Figure 2.

SEM images (a,b,e,f) and EDX analysis (c,d,g,h) of Zn micromotors. (a-d), Zn micromotors encapsulated with 500 nm SiO_2 particles: top view (a), side view (b), and EDX analysis (c, d). (e-h), control Zn micromotors without the SiO_2 particles. Top view (e), side view, (f) and EDX analysis (g, h). Scale bar, 0.5 μm (b,f), 1 μm (a,e), and 2 μm (c,d,g,h).

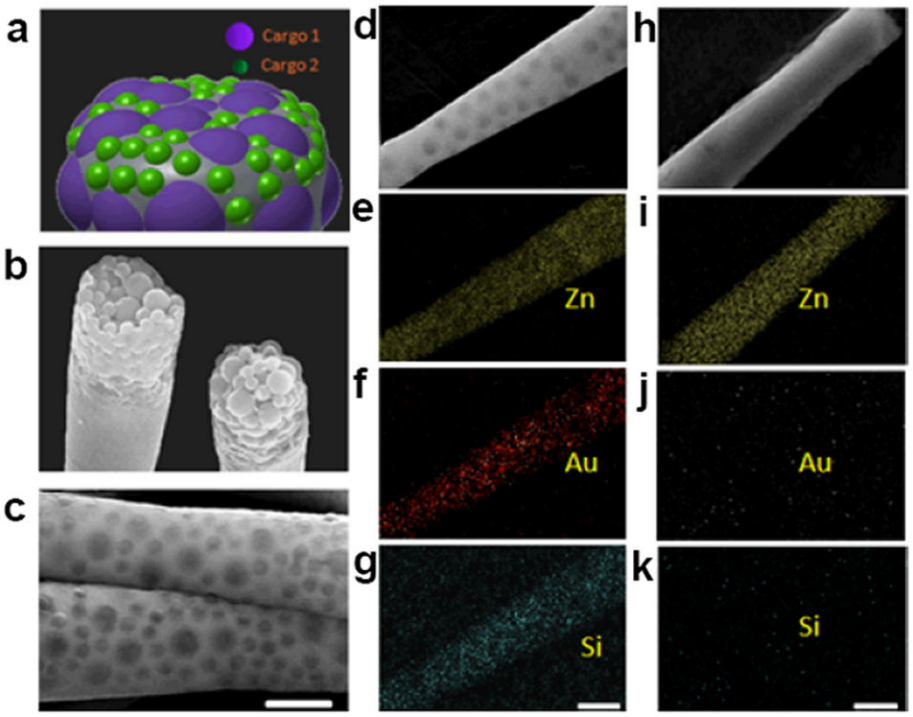

Figure 3.

Multi-cargo loaded micromotors. (a) Model depicts the encapsulation of different types of cargos, (b-c), SEM images display the top view (b) and side view (c) of the micromotors fully loaded with two differently sized SiO_2 particles (500 and 250 nm in diameter). (d-g), SEM image (d) and EDX analysis (e-g) of the micromotors fully loaded with both SiO_2 nanoparticles (500 nm) and Au nanoparticles (25 nm). (h-k), SEM image (h) and EDX analysis (i-k) of a control zinc micromotor without any particle loading. All scale bars, 1 μm.

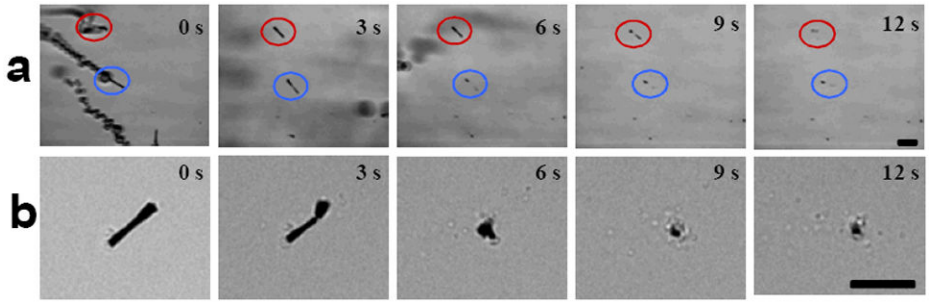

Figure 4.

Time-lapse images of the SiO_2–loaded micromotors. (a) Self-propulsion of multiple micromotors and autonomous cargo release in a 0.7 M HCl fuel solution. (b) Close-up images of the cargo release from a fully-loaded stationary micromotor in a 0.3 M HCl solution. Images (a) and (b) were taken at 3 s intervals from Movies S2 and S3, respectively. Scale bars, 20 μm.